

Dataset Augmentation by Mixing Visual Concepts

Abdullah Al Rahat, Hemanth Venkateswara
Georgia State University, USA

mkutubil@student.gsu.edu, hvenkateswara@gsu.edu

Abstract

This paper proposes a dataset augmentation method by fine-tuning pre-trained diffusion models. Generating images using a pre-trained diffusion model with textual conditioning often results in domain discrepancy between real data and generated images. We propose a fine-tuning approach where we adapt the diffusion model by conditioning it with real images and novel text embeddings. We introduce a unique procedure called Mixing Visual Concepts (MVC) where we create novel text embeddings from image captions. The MVC enables us to generate multiple images which are diverse and yet similar to the real data enabling us to perform effective dataset augmentation. We perform comprehensive qualitative and quantitative evaluations with the proposed dataset augmentation approach showcasing both coarse-grained and fine-grained changes in generated images. Our approach outperforms state-of-the-art augmentation techniques on benchmark classification tasks. The code is available at <https://github.com/rahatkutubi/MVC>

1. Introduction

Deep Neural Networks (DNNs) have achieved significant success due to their ability to learn complex representations from large datasets. However, they often require extensive data to prevent overfitting, which poses challenges in domains like visual recognition or medical imaging, where creating and annotating data such as MRI and X-ray images can be costly and time-consuming. Data augmentation is a key solution to this problem.

Data augmentation is used to increase the dataset size by generating new samples. Traditional image augmentation methods include geometric transformations (e.g., translation, rotation, affine transformations), color space transformations, kernel filters (e.g., blur, smoothing, sharpening), and image cropping [6]. Data augmentation techniques like AutoAugment [9], RandAugment [10], and geometric transformations of data are now an integral part of data pre-processing for training deep neural networks, and help in

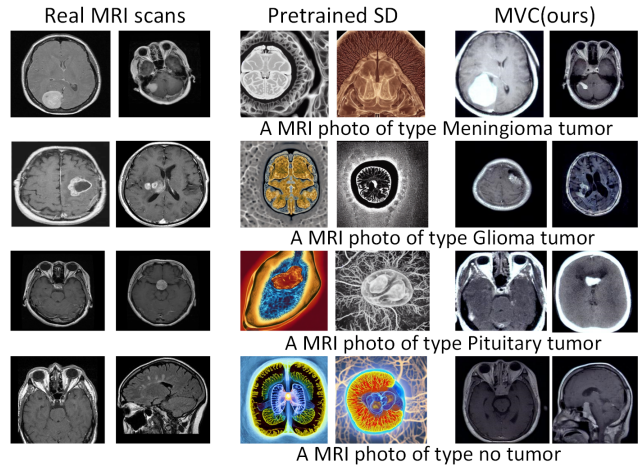


Figure 1. Naïvely deploying a pre-trained generative model to generate new images for dataset augmentation can lead to domain discrepancy. Columns 1, 2 are MRI scans from the Brain Tumor Dataset [5], Columns 3, 4 are images generated using a pre-trained Stable Diffusion (SD) model, Columns 5, 6 are images generated using the proposed MVC method.

avoiding overfitting. While these methods effectively increase dataset size, they lack natural variation as they are based on modifying existing data without introducing new concepts.

Recent advancements in deep generative models, such as Variational Autoencoders (VAE) [25], Generative Adversarial Networks (GAN) [16], Normalizing Flow [36], Autoregressive Models [46], and Diffusion models [19] have opened new avenues for generating synthetic data. These models can produce high-quality outputs such as realistic images, natural language, and diverse music and speech [13]. Among these, diffusion models have emerged as the most versatile approach to generate highly detailed, photo-realistic, and diverse samples, surpassing GANs and other models in quality and diversity. The rapid growth in research on diffusion models over the past two years highlights their potential for high-quality, diverse sample generation [7]. Notable examples include DALL-E 2 [35], Imagen [42], and Stable Diffusion [39], which have gained significant attention for their high-quality text-to-image generation capabilities.

Recent studies have demonstrated the effectiveness of synthetic images generated by generative diffusion models in classification tasks [18]. However, relying solely on pre-trained diffusion models that are conditioned by textual prompts from large language models can result in domain discrepancies between the real and generated data. In order to augment a dataset we propose to use image captions that can condition the diffusion model to generate images similar to the images in the dataset. This process is constrained to generate as many new images as the number of captions. But, can we not use a language model to generate additional similar captions? Yes, but that leads to domain discrepancy between generated and training data due to the variations in the new captions introduced by the language model. We therefore propose to work with caption embeddings rather than captions. In this work we introduce the technique of Mixing Visual Concepts (MVC) where we generate additional caption embeddings by mixing CLIP [34] generated embeddings of existing captions. We gain in three ways; (1) we are able to generate a large number of images, (2) the generated images are similar to the training data, and (3) we can control the diversity of the images by controlling the extent of mixing. Figure 1 compares the generated images produced by a pre-trained diffusion model and a fine-tuned diffusion model. It is evident that applying a pre-trained model naïvely without adaptation can lead to domain discrepancy in the augmented dataset.

Inspired by InstructPix2Pix [4], we condition a Stable Diffusion model [39] with novel caption embeddings to generate new images. We begin by generating captions for the images in our dataset using a vision-language model [30]. We apply the pre-trained CLIP to extract embeddings for these captions. We propose the MVC algorithm to generate novel embeddings by *mixing* the CLIP-generated embeddings. We fine-tune a pre-trained Stable Diffusion model [39] conditioned with novel caption embeddings along with the images in the dataset to generate new images for dataset augmentation. Our procedure generates images with distributional consistency and natural variations similar to real images. Our main contributions are as follows: (1) We introduce a robust dataset augmentation technique to generate within-domain data, (2) We demonstrate an efficient procedure to generate novel embeddings by mixing visual concepts (MVC) to condition the generative model, (3) We conduct extensive experiments to validate the effectiveness of the generated images on downstream classification tasks.

2. Related Work

Data augmentation techniques for image recognition are typically created manually, and the most effective methods are often tailored to specific datasets. For instance, elastic distortions, scaling, translation, and rotation are

commonly used for the MNIST dataset by top-performing models [26, 32, 37]. Meanwhile, random cropping, mirroring, and color shifting or whitening are more frequently employed for natural image datasets like CIFAR-10 and ImageNet [41]. However, these techniques require significant time and expert knowledge to develop [8].

There has been a notable shift in the field of data operations, with researchers now focusing on enhancing data by combining various strategies. For example, Smart Augmentation merges multiple samples from the same class to create innovative data networks [29]. Meanwhile, Tran et al. [45] utilize a Bayesian approach to generate augmented data based on the distribution learned from the training set. DeVries et al. [12] use noise, interpolations, and extrapolations in the feature space to enhance data.

In recent years AutoAugment [9] and RandAugment [10], have been extensively applied for dataset augmentation. They have been instrumental in achieving impressive results in image classification, self-supervised learning [17, 24, 36], and semi-supervised learning [3] on the ImageNet [41] benchmark. These augmentations are highly versatile and are particularly effective at encoding invariances to data transformations, making them a valuable tool for image classification. Methodologically, these find the best policies to group the primitive transformations to apply to real images in order to generate augmented images.

For image recognition tasks, additional datasets [14, 33, 38] are usually synthesized from a traditional simulation pipeline that uses a specific data source, such as synthetic 2D renderings of 3D models or scenes from graphics engines [18]. However, this approach has some drawbacks, including the potential for a discrepancy between distributions of the synthetic and real-world data, the need for large physical storage space, the high costs for sharing and transferring, and limitations in data amount and diversity due to using a specific data source [18]. On the other hand, generative models represent a more efficient approach to generating synthetic data, capable of producing high-fidelity, photorealistic images in large numbers.

Examples of attempts to use synthetic data from generative models for image recognition include a class-conditional Generative Adversarial Network (GAN) [2] to train classifiers for the same classes, and producing labels for object part segmentation [48] from the latent code of StyleGAN [23]. Although these works have shown promising results, they are limited in scope and focus on specific tasks [18]. On the other hand, Jahanian et al. [21] used a GAN-based generator to produce multiple views for unsupervised contrastive representation learning.

Shifting away from GAN-based augmentation, recent studies [43, 44] have highlighted the ability of diffusion models to generate training data with minimal or no examples, producing realistic training samples [22]. However, models trained solely on diffusion-generated data typically perform worse compared to those trained on real datasets, unless specifically fine-tuned for the target task [1, 44]. This is due to the domain gap between synthetically generated data and real data.

Our study aims to create augmentations that maintain visual consistency with the original training data. To achieve this, we explore blending micro concepts or characteristics from multiple images into generated images using engineered prompts in the CLIP [34] embedding space.

3. Method

3.1. Background and Preliminaries

Diffusion Model: A Denoising Diffusion Probabilistic Model (DDPM) [19] is a generative model that is designed to reverse (denoise) a diffusion process. The diffusion process gradually adds varying amounts of Gaussian noise $\epsilon \sim \mathcal{N}(0, I)$ to an input image x_0 over a specified number of timesteps $t \in \{1, 2, \dots, T\}$ until the resulting image is totally Gaussian noise. A diffused image x_t is obtained from input image x_0 based on the following equation,

$$x_t = \sqrt{\bar{\alpha}_t}x_0 + \sqrt{1 - \bar{\alpha}_t}\epsilon, \quad (1)$$

where $\bar{\alpha}_t = \prod_{i=1}^t \alpha_i$, and α_t is a time dependent noise scaling factor with $\alpha_1 = 1$ (no noise), and $\alpha_T \approx 0$ (only noise). The diffusion model is a denoiser neural network with parameters θ . It is trained to predict the noise ϵ diffused in the image. The parameters θ are estimated minimizing the following objective:

$$L = \min_{\theta} \mathbb{E}_{x_0, \epsilon, t} \|\epsilon - \epsilon_{\theta}(x_t, t)\|_2^2. \quad (2)$$

Starting with pure noise $x_T \sim \mathcal{N}(0, I)$, the denoiser network $\epsilon_{\theta}(x_t, t)$ predicts the noise in x_t . The noise is subtracted from x_t to transform it to x_{t-1} . This iterative procedure for $T \geq t \geq 1$ eventually yields the generated image x_0 .

Latent Diffusion Model (LDM): The LDM is an efficient diffusion model that performs diffusion and denoising in a reduced-dimensional latent space rather than in the high-dimensional pixel space [39]. A LDM trains an Autoencoder $D(E(x))$ to map an image x to a latent space, where $z \leftarrow E(x)$ is the latent representation and $E(\cdot)$ is the Encoder. The Decoder $D(\cdot)$ recreates the original image $\hat{x} \leftarrow D(z)$. In addition, the denoising process can be

conditioned to generate a desired image. The LDM is implemented as a time-conditioned U-Net [40] where cross-attention [39] is applied to integrate conditioning information into the denoising process to generate desired images. Conditioning information can be input in different modalities. For e.g. class labels, text prompts, segmentation maps, etc., are embedded into fixed-dimensional representations and input to the LDM denoiser to guide the denoising process. The objective function to train the LDM is,

$$L_{LDM} = \min_{\theta} \mathbb{E}_{z_0, \epsilon, t} \|\epsilon - \epsilon_{\theta}(z_t, t, e_{\mathcal{T}})\|_2^2, \quad (3)$$

where $e_{\mathcal{T}}$ is the embedded conditioning.

In case of dataset augmentation, we aim to keep the generated images similar to the images in the dataset. Inspired by the work in InstructPix2Pix [4], we modify the U-Net architecture in the LDM to leverage additional information in the form of image embedding $e_{\mathcal{I}} \leftarrow E(x)$. These embeddings are concatenated to the noisy latents z_t to condition the denoising process to generate images similar to x . Accordingly, we update the objective function as follows:

$$L_{LDM} = \min_{\theta} \mathbb{E}_{z_0, \epsilon, t} \|\epsilon - \epsilon_{\theta}(z_t, t, e_{\mathcal{T}}, e_{\mathcal{I}})\|_2^2. \quad (4)$$

During image generation, we first embed the noise image $x_T \sim \mathcal{N}(0, I)$ into the latent representation $z_T \leftarrow E(x_T)$. The denoiser network $\epsilon_{\theta}(z_t, t, e_{\mathcal{T}}, e_{\mathcal{I}})$ iteratively predicts the noise to transform z_t to z_{t-1} in the following manner,

$$z_{t-1} = \frac{1}{\sqrt{\alpha_t}} \left(z_t - \frac{1 - \alpha_t}{\sqrt{1 - \bar{\alpha}_t}} \epsilon_{\theta}(z_t, t, e_{\mathcal{T}}, e_{\mathcal{I}}) \right). \quad (5)$$

Arriving at z_0 , the decoder is applied to yield the generated image $\tilde{x} \leftarrow D(z_0)$. The text prompt embedding $e_{\mathcal{T}}$ and the image embedding $e_{\mathcal{I}}$ condition the generation process to yield desired images.

Classifier-free guidance: One of the key challenges in text-guided generation is the amplification of the effect induced by the conditioned text. To this end, Ho et al. [20] have presented the classifier-free guidance technique, where the denoising is also performed unconditionally, which is then extrapolated with the conditioned prediction. More formally, let $\emptyset = \psi(\cdot)$ be the embedding of a null text and let w be the guidance scale parameter, then the classifier-free guidance prediction is defined by:

$$\epsilon_{\theta}(z_t, t, e_{\mathcal{T}}, e_{\mathcal{I}}, \emptyset) = w \cdot \epsilon_{\theta}(z_t, t, e_{\mathcal{T}}, e_{\mathcal{I}}) + (1 - w) \cdot \epsilon_{\theta}(z_t, t, \emptyset), \quad (6)$$

where $w = 7.5$ is the default parameter for Stable Diffusion. We will now outline the procedure to create multiple embeddings by randomly mixing visual concepts from a limited set of embedded representations.

3.2. Mixing Visual Concepts

Consider all the K_y images $\{x_k^y\}_{k=1}^{K_y}$ belonging to a category y in the training dataset. It is our goal to generate N_y new images $\{\tilde{x}_k^y\}_{k=1}^{N_y}$ all with the same label y . We wish the generated images to be unique and yet ‘similar’ in style to the real images. We propose to achieve this by mixing visual concepts from multiple real images to generate a new image. We leverage the CLIP model which generates high-quality latent representations that effectively bridge visual and textual data [34].

Algorithm 1 Mixing Visual Concepts

Require: $\mathcal{C} := \{c_k\}_{k=1}^{K_y}$: Set of K_y Captions for category y , and $\text{CLIP}(\cdot)$: CLIP Text Embedder

- 1: $\mathcal{E} := \{e_k\}_{i=k}^{K_y}$ where $e_k \in \mathbb{R}^{m \times d}$ and $e_k \leftarrow \text{CLIP}(c_k)$
- 2: $\hat{\mathcal{E}} := \emptyset$ //set of mixed CLIP embeddings
- 3: **for** $k \leftarrow 1$ to N_y **do**
- 4: $\tilde{e}_k \leftarrow \text{RandSample}\{\mathcal{E}\}$
- 5: **for** $p \leftarrow 1$ to P **do** //Coarse mixing
- 6: $e_p \leftarrow \text{RandSample}\{\mathcal{E} \setminus \{\tilde{e}_k\}\}$
- 7: $r, s \leftarrow \text{Uniform}\{1, 2, \dots, m\}$ with $r < s$
- 8: $[\tilde{e}_k]_{r:s,:} \leftarrow [e_p]_{r:s,:}$ //replace rows $r:s$
- 9: **end for**
- 10: **for** $q \leftarrow 1$ to Q **do** //Fine mixing
- 11: $e_q \leftarrow \text{RandSample}\{\mathcal{E} \setminus \{\tilde{e}_k\}\}$
- 12: $u, v \leftarrow \text{Uniform}\{1, 2, \dots, d\}$ with $u < v$
- 13: $w \leftarrow \text{Uniform}\{1, 2, \dots, m\}$
- 14: $[\tilde{e}_k]_{w,u:v} \leftarrow [e_q]_{w,u:v}$ //replace $u:v$ in row w
- 15: **end for**
- 16: $\tilde{e}_k \leftarrow \tilde{e}_k \text{ } \textcircled{C} \text{ } \text{CLIP}(\emptyset)$ //Concat Class-free guidance
- 17: $\hat{\mathcal{E}} \leftarrow \hat{\mathcal{E}} \cup \{\tilde{e}_k\}$
- 18: **end for**

We begin with getting textual description/captions for the images using a pre-trained BLIP-2 model [30]. We prefix each caption with the sentence, ‘‘This is an image of $\langle y \rangle$ ’’ to ensure the category is captured in case the BLIP-2 model misses to label the image in the caption. This generates a set of captions, $\{c_k^y\}_{k=1}^{K_y}$. We arrive at the latent representations $\{e_k^y\}_{k=1}^{K_y}$ where $e \leftarrow \text{CLIP}(c)$ and $e \in \mathbb{R}^{m \times d}$. The CLIP embedding has a context of m tokens where each token is embedded in d dimensions. We propose to create new embeddings by mixing tokens from pre-existing embeddings. Starting with an embedding e_i , we replace some of its rows with corresponding rows from another embedding e_j . We term this *coarse mixing* when we make a relatively big edit to an embedding. We attempt to make fine changes to an embedding by replacing a few elements in the embedding with corresponding elements from other embeddings. We term this *fine mixing*. Algorithm 1

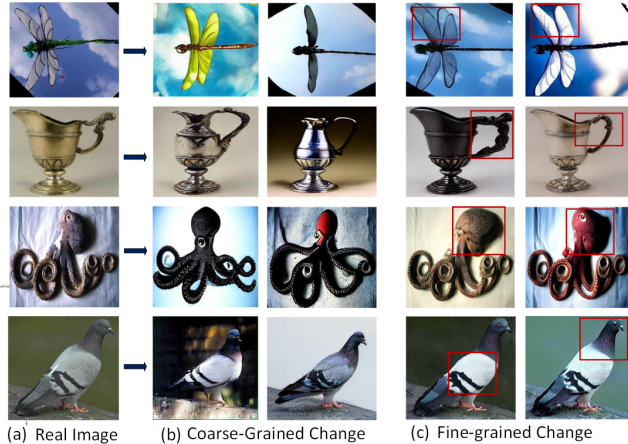


Figure 2. The results of coarse and fine mixing. (a) real image, (b) generated images conditioned on the real image along with coarse mixing, (c) generated images conditioned on the real image along with only fine mixing.

outlines the procedure to generate a set of new CLIP-like embeddings $\hat{\mathcal{E}}$ from pre-existing embeddings. Figure 2 displays the generated images with Coarse and Fine mixing.

3.3. Training and Generation

The new embeddings in $\hat{\mathcal{E}}$ are used to condition a diffusion model to generate new images similar to the images in the dataset.

Training: Figure 3 illustrates the fine-tuning process of the stable diffusion model with the training dataset. During training two images x and x' are selected at random from the same category y , for e.g., ‘Cat’. Their embeddings are estimated using a pre-trained encoder with $z_0 \leftarrow E(x)$ and $e_{\mathcal{I}} \leftarrow E(x')$. z_0 undergoes diffusion to yield a diffused latent z_t for $t \in \{1, 2, \dots, T\}$, according to Equation 1. The noise vector $\epsilon \sim \mathcal{N}(0, I)$ in Equation 1 is the size of the image latent z_0 . The other embedding $e_{\mathcal{I}}$ will play the role of image conditioning and will be concatenated with z_t . The pool of captions \mathcal{C} for the category y are used to generate new CLIP embeddings $\hat{\mathcal{E}}$ using Algorithm 1. These embeddings will be used as the text conditioning. $e_{\mathcal{T}} \in \hat{\mathcal{E}}$, $e_{\mathcal{I}}$ and z_t are used as input to the U-Net of the LDM $\epsilon_{\theta}(z_t, t, e_{\mathcal{T}}, e_{\mathcal{I}})$ to predict the noise ϵ_{θ} as per Equation 4 and train the parameters θ of the LDM using gradient descent. This procedure is repeated for images from every category and for all diffusion levels $t \in \{1, 2, \dots, T\}$.

Generation: The training yields the denoiser model $\epsilon_{\theta}(\cdot)$ which can predict the noise added to the latent image representation. During Generation, a noise vector $z_T \sim \mathcal{N}(0, I)$ is first sampled. To generate a new image for category y , for e.g., ‘Ewer’, an image x' from category y is selected at random and its embedding is obtained using the Encoder

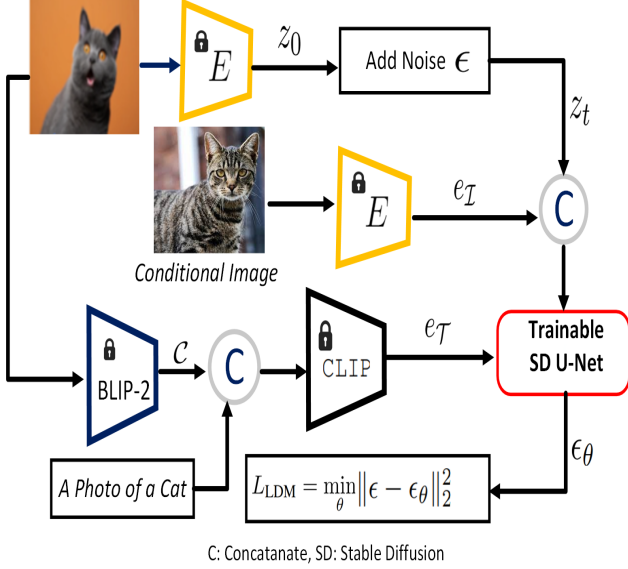


Figure 3. The training procedure illustrated with an image of a Cat: We fine-tune the pre-trained Stable Diffusion (SD U-Net) model. Input ‘Cat’ image is used to generate noisy latent z_t . The ‘Conditional Image’ is used to generate image conditioning e_I which is concatenated with z_t . Input image caption generated by BLIP-2, is concatenated with a user-provided prompt like for e.g., “a photo of a Cat”. The captions of all ‘Cat’ images are stored in \mathcal{C} and are used to generate text conditioning e_T with the MVC algorithm. The SD U-Net is trained using the objective in Equation 4.

$e_I \leftarrow E(x')$. e_I will play the role of image conditioning and will be concatenated with z_t . A new embedding $e_T \in \hat{\mathcal{E}}$ is sampled to play the role of text conditioning. e_T , e_I and z_T are used as input to the trained U-Net of the LDM $\epsilon_\theta(z_T, t, e_T, e_I)$ to predict the noise as per Equation 4. The predicted noise ϵ_θ is used to estimate the denoised latent z_{T-1} using Equation 5. This procedure is iterated for $T \geq t \geq 1$ using the same embeddings e_T and e_I to obtain the completely denoised latent z_0 . The pre-trained Decoder is used to generate the new image from the denoised latent with $\hat{x} \leftarrow D(z_0)$. Figure 4 outlines the procedure for synthesizing new samples in a dataset.

Besides generating samples from our proposed methods, we use the pre-trained text-to-image diffusion model to generate new samples using the caption of images from the training dataset. For special domains like medical datasets, relying solely on pre-trained models may not be effective. However, for more general-purpose datasets such as ImageNet [11], pre-trained models can provide additional diversity and variability in generated samples. For CIFAR-10 and CIFAR-100, we generate additional images using a pre-trained Stable Diffusion (SD) model.

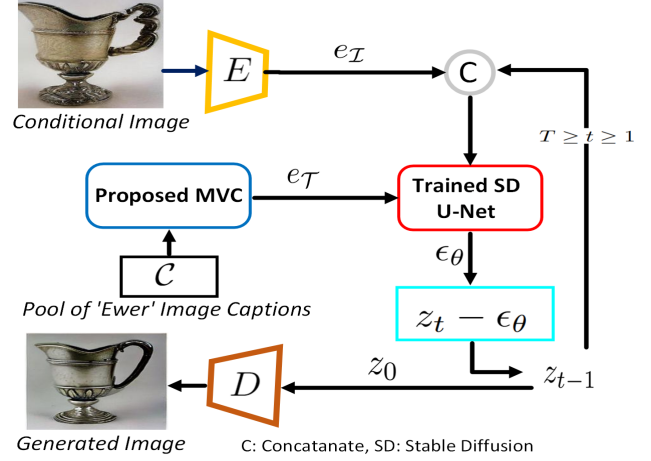


Figure 4. An overview of image generation: We begin with a complete noisy latent $z_T \sim \mathcal{N}(0, I)$. To generate an ‘Ewer’-like image we use the Conditional Image to generate an image embedding e_I and concatenate it with z_T . We apply the MVC algorithm on the pool of image captions of ‘Ewer’ to obtain the text conditioning e_T . We apply the denoising procedure in Equation 5 to estimate z_{T-1} from z_T . We iterate this procedure for $T \geq t \geq 1$ to arrive at z_0 - the denoised latent. We apply the decoder to obtain the new image $\hat{x} \leftarrow D(z_0)$.

4. Experiments and Results

Stable Diffusion. Stable Diffusion (SD) [39] is a cutting-edge text-to-image model that generates photorealistic images from text prompts. It is a conditional diffusion model, progressively refining noisy samples into realistic images that match the input text’s visual context. We adopt the pre-trained SD model for text-to-image generation. We fine-tune its U-Net component to accept images from the training dataset and a prompt as conditioning inputs.

Our image augmentation process combines both our fine-tuned and a pre-trained SD model, effectively enhancing data for general classification tasks. However, for specialized domains such as medical image datasets (e.g., MRI, X-ray, CT scans), we rely exclusively on our trained SD model. This choice is due to limitations in pre-trained models’ ability to accurately generate medical images, which often lack sufficient representation of medical data in their training sets. Our trained SD model excels in producing new medical images with diverse variations. To generate these images, we employ the proposed MVC procedure to generate novel text embeddings using image captions as prompts, which integrates concepts and contexts from multiple images via text embedding. Algorithm 1 outlines the MVC procedure.

Datasets. To explore the space of data augmentations, we experiment with core image classification datasets such as CIFAR-10 and CIFAR-100 [27], which are commonly used benchmarks in the field. These datasets enable direct comparisons with prior research. We also consider Tiny Im-

Table 1. Test accuracy (%) on Tiny ImageNet [28] CIFAR-10, CIFAR-100 and their reduced sets. Comparisons across default data augmentation (baseline), and Fast AutoAugment (Fast AA) [31], AutoAugment (AA) [9] and RandAugment (RA) [10] and proposed approach (Ours). We reuse baseline results from the AA and RA paper, and results marked with * are reproduced using the same settings. The Results reported by us are averaged over 3 independent runs. The green color indicates the percent improvement from the corresponding baseline.

Model	Baseline	FAA	AA	RA	Ours(Syn)	Ours(FAA+Syn)	Ours(AA+Syn)	Ours(RA+Syn)
CIFAR-10								
Wide-ResNet-28-2	94.9	95.9*	95.9	95.8	95.6(+0.7)	96.2(+0.3)	96.3(+0.4)	96.6(+0.8)
Wide-ResNet-28-10	96.1	97.3	97.4	97.3	96.5(+0.4)	97.6(+0.3)	97.6(+0.2)	97.7(+0.4)
CIFAR-10 Reduced								
Wide-ResNet-28-2	79.5*	83.8*	83.7*	83.9*	82.9(+3.4)	86.2(+2.4)	86.6(+2.9)	86.4(+2.5)
Wide-ResNet-28-10	81.2	85.9*	86.1	85.6*	85.1(+3.9)	87.4(+1.5)	87.3(+1.2)	87.5(+1.9)
CIFAR-100								
Wide-ResNet-28-2	75.4	78.7*	78.5	78.3	76.9(+1.5)	80.7(+2.0)	80.4(+1.9)	81.5(+3.2)
Wide-ResNet-28-10	81.2	82.7	82.4	82.9	83.3(+2.1)	84.5(+1.8)	84.4(+1.5)	84.9(+1.6)
CIFAR-100 Reduced								
Wide-ResNet-28-2	39.7*	45.4*	44.7*	44.8*	46.1(+6.4)	47.7(+2.3)	47.5(+2.8)	47.8(+3.0)
Wide-ResNet-28-10	41.5*	46.3*	45.9*	45.7*	47.8(+6.3)	48.7(+2.4)	48.1(+2.2)	48.5(+2.8)
Tiny ImageNet								
ResNet50	27.3*	30.5*	30.4*	-	33.2(+5.9)	35.4(+2.3)	35.5(+2.8)	-
EfficientNet-b3	46.3*	-	-	47.9*	48.6(+2.3)	-	-	49.4(+2.8)
Average	-	-	-	-	(+3.29)	(+1.70)	(+1.77)	(+2.11)

Table 2. Test accuracy (%) on Caltech101 datasets [15]. Comparisons across default data augmentation (baseline), AutoAugment (AA) [9], RandAugment (RA) [10] and proposed approach (Ours). All of the Results are reported by us averaging over 3 independent runs. The green color indicates the percent improvement from the corresponding baseline.

Model	Baseline	AA	RA	Ours(AA+Syn)	Ours(RA+Syn)
RestNet50	95	96.1	96.4	97.2(+1.1)	97.5(+1.1)
EfficientNet-b0	95.2	95.1	95.5	95.8(+0.7)	96.3(+0.8)
VIT-16	96.2	96.7	96.9	97.5(+0.8)	97.9(+1.0)
Average	-	-	-(+0.3)	(+0.87)	(+0.97)

ageNet [28], one of the harder datasets in the classification task. In addition, we include medical image datasets [5] to broaden our experimentation scope, highlighting the benefits of augmented images in training compared to traditional augmentation methods. Furthermore, we explore the Caltech-101 dataset [15], renowned for its fine-grained classification challenges. We reorganize the training dataset by randomly selecting pairs of images with the same class label and pairing them to fine-tune the SD model. Details of data preparation are discussed in the Supplementary.

Training. For fine-tuning the SD model, we adopt an end-to-end training approach inspired by InstructPix2Pix [4] using our curated source dataset. Similar to current augmentation techniques [9, 10, 31], the training of a classification model for CIFAR-10 and CIFAR-100 datasets starts from scratch with similar hyperparameter settings. Tiny ImageNet: we choose a learning rate of 10^{-3} and 50 epochs for ResNet50. For EfficientNet-B3, we use a learning rate of 10^{-2} and 20 epochs. We select a batch size of 128 for both models. Caltech101: we choose a learning rate of 10^{-4} with an ADAM optimizer. For Brain Tumor Dataset, different hyperparameter settings are selected for various classification models, with details provided in the Supple-

mentary.

4.1. Results

CIFAR-10 and CIFAR-100 Results. In Table 1, we present the test set accuracy for different neural network architectures. We implemented the Wide-ResNet-28-2 and Wide-ResNet-28-10 [47] models in PyTorch and used the same model and hyperparameter settings to evaluate the test set accuracy. As shown in the Table 1, we achieved an average accuracy improvement of 3.29%, 1.70%, 1.77%, and 2.11% compared to Baseline, FastAutoAugment, AutoAugment, and RandAugment respectively. Similar to AutoAugment, we trained on 4,000 labeled examples randomly sampled from the CIFAR-10 dataset, which we referred to as CIFAR-10 Reduced and CIFAR-100 Reduced.

Fine-grained Classification Result. The effectiveness of diffusion model augmentation in the fine-grained domain was investigated using the Caltech101 dataset [15]. This dataset presents a challenge due to its imbalanced nature and relatively small training sets, despite containing numerous classes. In Table 2, the classification results show that our methods outperformed the baseline, AutoAugment and RandAugment by a significant margin.

Table 3. Test accuracy (%) on Brain Tumor Dataset [5]. Comparisons across, AutoAugment (AA) [9], RandAugment(RA) [10] and proposed approach (Ours). All of the Results are reported by us averaging over 3 independent runs. The green color indicates the percent improvement from the corresponding baseline.

Model	Baseline	AA	RA	Ours(AA+Syn)	Ours(RA+Syn)
RestNet50	93.2	94.4	95.6	96.1(+1.7)	96.8(+1.2)
EfficientNet-B0	91.9	93.3	94.5	95.2(+1.9)	95.2(+0.7)
Wide-RestNet-50-2	92.3	94.7	95.6	95.8(+1.1)	96.7(+1.1)
Average	-	-	-	(+1.43)	(+1.13)

Medical Image Dataset Results. Medical images differ significantly from images in other fields. Moreover, obtaining real MRI or CT scan datasets can be challenging due to the high cost and limited availability of patients. Therefore, data augmentation is a common necessity in the medical field. We assessed our proposed MVC method for augmentation in the medical domain and the classification accuracy results are presented in Table 3, showing a 1.43% and 1.13% improvement compared to state-of-the-art methods. We note that as the size of the training set increases, the impact of data augmentation is expected to diminish. We observed that for CIFAR-10 and the reduced set CIFAR-100, we achieved a greater improvement in percentages compared to the full set.

4.2. Ablation Study

4.2.1 Is Diversity Enough?

Our study investigated the impact of image data augmentation on classification accuracy. We observed that enhancing diversity alone doesn't consistently improve classification results unless out-of-domain sample generation is carefully managed. Specifically, when utilizing pre-trained diffusion models, such as stable diffusion, we found that the samples generated often deviated significantly from the dataset's domain. This effect was particularly pronounced in fine-grained datasets like Caltech101 and specialized domains such as MRI, X-ray, and CT-SCAN. Figure 1 illustrates the limitations of pre-trained SD models in the medical domain. However, there are cases where pre-trained SD models can produce diverse samples that align well with the dataset. For instance, in Figure 5, the last row demonstrates diversified augmented samples derived from CIFAR-100.

Need for Fine-Tuning and Guided Augmentation. To address pre-trained model challenges, our research emphasizes fine-tuning diffusion models for fine-grain and medical imaging datasets. Fine-tuning allows models to adjust generation capabilities to better match dataset characteristics, improving sample quality and relevance. We stress the importance of a tailored augmentation prompting algorithm to guide sample generation, aligning outputs with domain-specific features. Table 4 illustrates the effect of using a pre-trained and fine-tuned SD model on test accuracy, and it also presents the average accuracy improvement for the fine-tuned setting. Additionally, Figure 6 illustrates how

Table 4. Impact of Pre-trained (PT) vs fine-tuned (FT) SD model on test accuracy (%) on Caltech101, CIFAR100, and Brain Tumor Dataset. Comparisons across AutoAugment (AA) [9] + Synthetic Data from Pre-trained [39] and Fine-tuned SD Model [4].

Model	AA	AA+Syn(PT)	AA+Syn(FT)
Caltech101			
RestNet50	96.1	96.8(+0.7)	97.2(+1.1)
EfficientNet-B0	95.1	95.6(+0.5)	95.8(+0.7)
VIT-16	96.7	97.3(+0.6)	97.5(+0.8)
CIFAR100 Reduced			
Wide-ResNet-28-2	44.7	46.1(+01.4)	47.3(+2.6)
Brain Tumor Dataset			
ResNet50	94.4	-	96.1(+1.7)
Average	-	(+0.8)	(+1.38)

concept mixing influences the diversity of augmented images created using the proposed MVC method. It combines color and shape concepts from multiple real images into augmented images. However, generated images from a pretrained model look more diverse, but they exhibit some moderate deviation from in domain distribution which may affect model learning.

4.2.2 Effective Training Strategy

Learning from Image-Caption Pairs. We initially trained the diffusion model with paired image-caption data. This method focused on teaching the model to generate images based on specific textual descriptions of images. While effective in reinforcing direct associations between images and captions, its ability to generate diverse outputs beyond paired examples was limited.

Generating Diverse In-domain Samples. In the second approach, we created a dataset pairing images and captions randomly selected from the same class label. This method aimed to broaden the model's capacity to generate diverse images within the context of specific class labels. This approach yielded superior results compared to the first method. It enhanced the model's ability to produce varied but contextually relevant images within defined domains.

Impact of Synthetic Data Quantity. In our exploration of integrating augmented synthetic datasets to train classification models, we tested three different approaches. Initially, we found that simply adding the synthetic dataset to the real

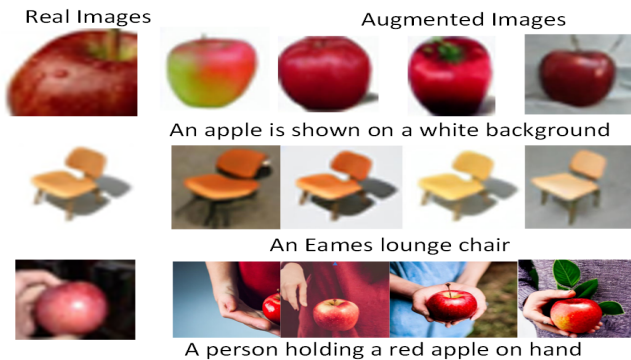


Figure 5. Column 1 depicts real images from CIFAR-100. In the remaining columns, the first two rows are images generated using the proposed MVC method, which constrains generated images to be in-domain. The third row represents images generated using a pre-trained SD model, which provides more diversity with no control over in-domain generation.

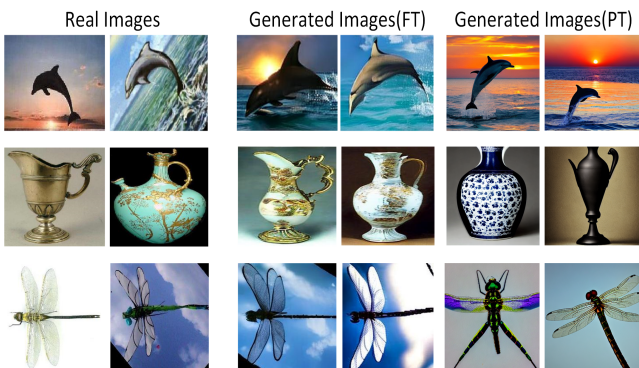


Figure 6. The impact of concept mixing on augmented images that were created using the MVC method. The first two images on the left side represent the original images from the Caltech101 dataset, while the subsequent images are the generated ones from fine tuned DM and pretrained DM.

training dataset did not significantly boost classification accuracy. This approach proved ineffective, especially when the synthetic dataset outnumbered the real dataset by a large margin, leading to a noticeable bias towards the synthetic data. This bias occurred because the model had more exposure to synthetic examples, potentially overshadowing the patterns present in the real data. Later we tested two other strategies. two-phase training and Random Selection with Probability (RSP).

Two-phase Training: In the first phase, we trained the classification models using a combined dataset. This dataset included both real and synthetic data, with the synthetic data being three to four times larger than the real data. During this phase, the model focused on learning general patterns and features present in both types of data. Exposure to a large volume of synthetic data helped the model understand the wider range of possible inputs. After the initial training phase, we fine-tuned the model using only the real dataset, with reduced training steps and a smaller learning

Table 5. Impact of different training strategies on test accuracy (%) on Caltech101 Dataset. Comparisons across AutoAugment (AA) [9], combined (real+synthetic), Random Selection with Probability (RSP) and two-phase training strategies.

Model	AA	combined	RSP	Two-Phase
RestNet50	96.1	95.4(-0.7)	96.3	97.2(+1.1)
EfficientNet-B0	95.1	94.9(-0.2)	95.3	95.8(+0.7)
VIT-16	96.7	97.2(+0.5)	97.2	97.5(+0.8)

rate. This phase aimed to refine the model’s understanding specifically on real-world examples. By limiting the number of training iterations during fine-tuning, we prevented the model from overfitting to the real dataset.

Random Selection with Probability (RSP): This method involved randomly selecting synthetic images with a specified probability (e.g., 80%) from a pool of synthetic datasets and integrating them with batches from the real dataset during training. This approach aimed to dynamically balance the integration of synthetic and real data to enhance training effectiveness. Table 5 compares the different training approaches where we see two-phase training outperformed others. Training strategies are given in the Supplementary.

5. Conclusion

Our experiments demonstrate that synthetic data significantly improves classifier learning. However, we identified limitations with pre-trained diffusion models. Despite their general capability to produce high-quality samples, pre-trained diffusion models struggle when it comes to aligning with specific dataset domains, such as fine-grained classification and medical images, likely due to inherent training biases. This lack of alignment can lead to sub-optimal performance and decreased effectiveness in these specialized domains. To address these limitations, we emphasize the critical role of fine-tuning and domain-specific augmentation strategies in mitigating out-of-domain sample generation issues. Our proposed fine-tuning strategies and MVC method are crucial to enhance the quality and applicability of generated samples in specialized domains, ultimately improving the effectiveness of machine learning models in real-world applications.

6. Acknowledgment

This research was sponsored by the Army Research Laboratory and was accomplished under Cooperative Agreement Number W911NF-23-2-0224. The views and conclusions contained in this document are those of the authors and should not be interpreted as representing the official policies, either expressed or implied, of the Army Research Laboratory or the U.S. Government. The U.S. Government is authorized to reproduce and distribute reprints for Government purposes notwithstanding any copyright notation herein.

References

- [1] Shekoofeh Azizi, Simon Kornblith, Chitwan Saharia, Mohammad Norouzi, and David J Fleet. Synthetic data from diffusion models improves imagenet classification. *arXiv preprint arXiv:2304.08466*, 2023. [3](#)
- [2] Victor Besnier, Himalaya Jain, Andrei Bursuc, Matthieu Cord, and Patrick Pérez. This dataset does not exist: training models from generated images. In *ICASSP 2020-2020 IEEE International Conference on Acoustics, Speech and Signal Processing (ICASSP)*, pages 1–5. IEEE, 2020. [2](#)
- [3] Sam Bond-Taylor, Adam Leach, Yang Long, and Chris G Willcocks. Deep generative modelling: A comparative review of vaes, gans, normalizing flows, energy-based and autoregressive models. *IEEE transactions on pattern analysis and machine intelligence*, 2021. [2](#)
- [4] Tim Brooks, Aleksander Holynski, and Alexei A Efros. Instructpix2pix: Learning to follow image editing instructions. In *Proceedings of the IEEE/CVF Conference on Computer Vision and Pattern Recognition*, pages 18392–18402, 2023. [2](#), [3](#), [6](#), [7](#)
- [5] Jyotismita Chaki and Marcin Wozniak. Brain tumor mri dataset, 2023. [1](#), [6](#), [7](#)
- [6] Phillip Chlap, Hang Min, Nym Vandenberg, Jason Dowling, Lois Holloway, and Annette Haworth. A review of medical image data augmentation techniques for deep learning applications. *Journal of Medical Imaging and Radiation Oncology*, 65(5):545–563, 2021. [1](#)
- [7] Florinel-Alin Croitoru, Vlad Hondru, Radu Tudor Ionescu, and Mubarak Shah. Diffusion models in vision: A survey. *IEEE Transactions on Pattern Analysis and Machine Intelligence*, 2023. [1](#)
- [8] Ekin D Cubuk, Barret Zoph, Dandelion Mane, Vijay Vasudevan, and Quoc V Le. Autoaugment: Learning augmentation policies from data. *arXiv preprint arXiv:1805.09501*, 2018. [2](#)
- [9] Ekin D Cubuk, Barret Zoph, Dandelion Mane, Vijay Vasudevan, and Quoc V Le. Autoaugment: Learning augmentation strategies from data. In *Proceedings of the IEEE/CVF conference on computer vision and pattern recognition*, pages 113–123, 2019. [1](#), [2](#), [6](#), [7](#), [8](#)
- [10] Ekin D Cubuk, Barret Zoph, Jonathon Shlens, and Quoc V Le. Randaugment: Practical automated data augmentation with a reduced search space. In *Proceedings of the IEEE/CVF conference on computer vision and pattern recognition workshops*, pages 702–703, 2020. [1](#), [2](#), [6](#), [7](#)
- [11] Jia Deng, Wei Dong, Richard Socher, Li-Jia Li, Kai Li, and Li Fei-Fei. Imagenet: A large-scale hierarchical image database. In *2009 IEEE conference on computer vision and pattern recognition*, pages 248–255. Ieee, 2009. [5](#)
- [12] Terrance DeVries and Graham W Taylor. Dataset augmentation in feature space. *arXiv preprint arXiv:1702.05538*, 2017. [2](#)
- [13] Prafulla Dhariwal, Heewoo Jun, Christine Payne, Jong Wook Kim, Alec Radford, and Ilya Sutskever. Jukebox: A generative model for music. *arXiv preprint arXiv:2005.00341*, 2020. [1](#)
- [14] Alexey Dosovitskiy, Philipp Fischer, Eddy Ilg, Philip Hausser, Caner Hazirbas, Vladimir Golkov, Patrick Van Der Smagt, Daniel Cremers, and Thomas Brox. FlowNet: Learning optical flow with convolutional networks. In *Proceedings of the IEEE international conference on computer vision*, pages 2758–2766, 2015. [2](#)
- [15] Li Fei-Fei, Robert Fergus, and Pietro Perona. One-shot learning of object categories. *IEEE transactions on pattern analysis and machine intelligence*, 28(4):594–611, 2006. [6](#)
- [16] Ian Goodfellow, Jean Pouget-Abadie, Mehdi Mirza, Bing Xu, David Warde-Farley, Sherjil Ozair, Aaron Courville, and Yoshua Bengio. Generative adversarial nets. *Advances in neural information processing systems*, 27, 2014. [1](#)
- [17] Jie Gui, Zhenan Sun, Yonggang Wen, Dacheng Tao, and Jieping Ye. A review on generative adversarial networks: Algorithms, theory, and applications. *IEEE transactions on knowledge and data engineering*, 35(4):3313–3332, 2021. [2](#)
- [18] Ruifei He, Shuyang Sun, Xin Yu, Chuhui Xue, Wenqing Zhang, Philip Torr, Song Bai, and Xiaojuan Qi. Is synthetic data from generative models ready for image recognition? *arXiv preprint arXiv:2210.07574*, 2022. [2](#)
- [19] Jonathan Ho, Ajay Jain, and Pieter Abbeel. Denoising diffusion probabilistic models. *Advances in neural information processing systems*, 33:6840–6851, 2020. [1](#), [3](#)
- [20] Jonathan Ho and Tim Salimans. Classifier-free diffusion guidance. *arXiv preprint arXiv:2207.12598*, 2022. [3](#)
- [21] Ali Jahani, Xavier Puig, Yonglong Tian, and Phillip Isola. Generative models as a data source for multiview representation learning. *arXiv preprint arXiv:2106.05258*, 2021. [2](#)
- [22] Saachi Jain, Hannah Lawrence, Ankur Moitra, and Aleksander Madry. Distilling model failures as directions in latent space. *arXiv preprint arXiv:2206.14754*, 2022. [3](#)
- [23] Tero Karras, Samuli Laine, and Timo Aila. A style-based generator architecture for generative adversarial networks. In *Proceedings of the IEEE/CVF conference on computer vision and pattern recognition*, pages 4401–4410, 2019. [2](#)
- [24] Taesup Kim and Yoshua Bengio. Deep directed generative models with energy-based probability estimation. *arXiv preprint arXiv:1606.03439*, 2016. [2](#)
- [25] Diederik P Kingma and Max Welling. Auto-encoding variational bayes. *arXiv preprint arXiv:1312.6114*, 2013. [1](#)
- [26] Diederik P Kingma, Max Welling, et al. An introduction to variational autoencoders. *Foundations and Trends® in Machine Learning*, 12(4):307–392, 2019. [2](#)
- [27] Alex Krizhevsky, Geoffrey Hinton, et al. Learning multiple layers of features from tiny images. 2009. [5](#)
- [28] Ya Le and Xuan Yang. Tiny imagenet visual recognition challenge. *CS 231N*, 7(7):3, 2015. [6](#)
- [29] Joseph Lemley, Shabab Bazrafkan, and Peter Corcoran. Smart augmentation learning an optimal data augmentation strategy. *Ieee Access*, 5:5858–5869, 2017. [2](#)
- [30] Junnan Li, Dongxu Li, Silvio Savarese, and Steven Hoi. Blip-2: Bootstrapping language-image pre-training with frozen image encoders and large language models. In *International conference on machine learning*, pages 19730–19742. PMLR, 2023. [2](#), [4](#)

- [31] Sungbin Lim, Ildoo Kim, Taesup Kim, Chiheon Kim, and Sungwoong Kim. Fast autoaugment. *Advances in neural information processing systems*, 32, 2019. 6
- [32] Jiquan Ngiam, Zhenghao Chen, Pang W Koh, and Andrew Y Ng. Learning deep energy models. In *ICML*, pages 1105–1112, 2011. 2
- [33] Xingchao Peng, Ben Usman, Neela Kaushik, Judy Hoffman, Dequan Wang, and Kate Saenko. Visda: The visual domain adaptation challenge. *arXiv preprint arXiv:1710.06924*, 2017. 2
- [34] Alec Radford, Jong Wook Kim, Chris Hallacy, Aditya Ramesh, Gabriel Goh, Sandhini Agarwal, Girish Sastry, Amanda Askell, Pamela Mishkin, Jack Clark, et al. Learning transferable visual models from natural language supervision. In *International conference on machine learning*, pages 8748–8763. PMLR, 2021. 2, 3, 4
- [35] Aditya Ramesh, Prafulla Dhariwal, Alex Nichol, Casey Chu, and Mark Chen. Hierarchical text-conditional image generation with clip latents. *arXiv preprint arXiv:2204.06125*, 1(2):3, 2022. 1
- [36] Danilo Rezende and Shakir Mohamed. Variational inference with normalizing flows. In *International conference on machine learning*, pages 1530–1538. PMLR, 2015. 1, 2
- [37] Danilo Jimenez Rezende, Shakir Mohamed, and Daan Wierstra. Stochastic backpropagation and approximate inference in deep generative models. In *ICML*, pages 1278–1286. PMLR, 2014. 2
- [38] Stephan R Richter, Vibhav Vineet, Stefan Roth, and Vladlen Koltun. Playing for data: Ground truth from computer games. In *Computer Vision–ECCV 2016: 14th European Conference, Amsterdam, The Netherlands, October 11–14, 2016, Proceedings, Part II 14*, pages 102–118. Springer, 2016. 2
- [39] Robin Rombach, Andreas Blattmann, Dominik Lorenz, Patrick Esser, and Björn Ommer. High-resolution image synthesis with latent diffusion models. In *Proceedings of the IEEE/CVF conference on computer vision and pattern recognition*, pages 10684–10695, 2022. 1, 2, 3, 5, 7
- [40] Olaf Ronneberger, Philipp Fischer, and Thomas Brox. U-net: Convolutional networks for biomedical image segmentation. In *Medical Image Computing and Computer-Assisted Intervention–MICCAI 2015: 18th International Conference, Munich, Germany, October 5–9, 2015, Proceedings, Part III 18*, pages 234–241. Springer, 2015. 3
- [41] Olga Russakovsky, Jia Deng, Hao Su, Jonathan Krause, Sanjeev Satheesh, Sean Ma, Zhiheng Huang, Andrej Karpathy, Aditya Khosla, Michael Bernstein, et al. Imagenet large scale visual recognition challenge. *International journal of computer vision*, 115:211–252, 2015. 2
- [42] Chitwan Saharia, William Chan, Saurabh Saxena, Lala Li, Jay Whang, Emily L Denton, Kamyar Ghasemipour, Raphael Gontijo Lopes, Burcu Karagol Ayan, Tim Salimans, et al. Photorealistic text-to-image diffusion models with deep language understanding. *Advances in Neural Information Processing Systems*, 35:36479–36494, 2022. 1
- [43] Jordan Shipard, Arnold Wiliem, Kien Nguyen Thanh, Wei Xiang, and Clinton Fookes. Boosting zero-shot classification with synthetic data diversity via stable diffusion. *arXiv preprint arXiv:2302.03298*, 2023. 3
- [44] Brandon Trabucco, Kyle Doherty, Max Gurinas, and Ruslan Salakhutdinov. Effective data augmentation with diffusion models. *arXiv preprint arXiv:2302.07944*, 2023. 3
- [45] Toan Tran, Trung Pham, Gustavo Carneiro, Lyle Palmer, and Ian Reid. A bayesian data augmentation approach for learning deep models. *Advances in neural information processing systems*, 30, 2017. 2
- [46] Aaron Van den Oord, Nal Kalchbrenner, Lasse Espeholt, Oriol Vinyals, Alex Graves, et al. Conditional image generation with pixelcnn decoders. *Advances in neural information processing systems*, 29, 2016. 1
- [47] Sergey Zagoruyko and Nikos Komodakis. Wide residual networks. In *Proceedings of the British Machine Vision Conference 2016, BMVC*. BMVA Press, 2016. 6
- [48] Yuxuan Zhang, Huan Ling, Jun Gao, Kangxue Yin, Jean-Francois Lafleche, Adela Barriuso, Antonio Torralba, and Sanja Fidler. Datasetgan: Efficient labeled data factory with minimal human effort. In *Proceedings of the IEEE/CVF Conference on Computer Vision and Pattern Recognition*, pages 10145–10155, 2021. 2